OPEN ACCESS
JOURNAL OF ADVANCED DIELECTRICS
Vol. 11, No. 5 (2021) 2160001 (5 pages)

DOI: 10.1142/S2010135X21600018

Features of the electrophysical and mechanical properties of *n*-component ferroactive solid solutions of composition PZT–PZN–PMN

K. P. Andryushin*,§, I. N. Andryushina*, A. V. Cherpakov†, A. V. Popov‡,
I. A. Verbenko* and L. A. Reznichenko*

*Research Institute of Physics, Southern Federal University,
Rostov-on-Don 344090, Stachki str. 194, Russia

†Institute of Mathematics, Mechanics, and Computer Science named after of I.I. Vorovich
Southern Federal University Rostov-on-Don 344090, Stachki str. 200/1, Russia

‡Institute of Mathematics, Mechanics and Computer Science
Southern Federal University, Rostov-on-Don 344090
Milchakova 8a, Russia

§kpandryushin@gmail.com

Received 25 April 2021; Accepted 14 May 2021; Published 11 June 2021

Study of the fatigue endurance and mechanical strength of solid solutions of the PZT–PZN–PMN system, modified with Ba and Sr, corresponding to the formula $(Pb_{1-\alpha_1-\alpha_2}Sr_{\alpha_1}Ba_{\alpha_1})$ $[Ti_xZr_y\langle(Nb_{2/3}Zn_{1/3})$ $(Nb_{2/3}Mg_{1/3})\rangle_{1-x-y}]O_3$, with $\alpha_1 = 0.02 \div 0.12$; $\Delta\alpha_1 = 0.02$, $\alpha_2 = 0.0036 \div 0.073$; $x = 0.385 \div 0.430$, $y = 0.402 \div 0.447$ is presented. It is shown that the evolution of the polarization characteristics with an increase in the number of repolarization cycles, n, is characterized by two sections: slow fatigue and logarithmic evolution. It was found that an increase in the strontium content shifts the beginning of the logarithmic stage towards to the large n. It is shown that an increase in the average grain size decreases the mechanical strength. A conclusion is made about the expediency of using the obtained data in the development of devices operating in power modes.

Keywords: PZT–PZN–PMN; *P–E* loops; fatigue endurance; mechanical properties.

1. Introduction

The basis of the most common solid solutions (SS) used in the production of ferroactive components for filters, sensors, ultrasonic motors, etc. is the system of lead zirconate titanate $PbZrO_3$–$PbTiO_3$, PZT.[1–6] This is due to the high Curie temperature and piezoelectric constants of SS in the morphotropic region (MR) (the region of the structural phase transition, accompanied by extrema of the electrophysical characteristics). However, despite the obvious advantages of the PZT system, its capabilities were practically exhausted by the 70s of the last century. To overcome the difficulties that have arisen, the transition to multicomponent systems was carried out, in which the dimensionality of the MR increases, which significantly expands the range of compositions with various properties, the possibility of choosing SS with a given combination of parameters, and also increases their efficiency and manufacturability.[7–17]

One of such system is the PZT–PZN–PMN[18–21] designed for low frequency applications. Earlier, for a number of the specified composition, the structure, microstructure, electrical properties were investigated in a wide range of temperatures and external electric fields.

It should be noted that in the development of such materials, the main attention was paid to the study of their dielectric, piezoelectric, and ferroelastic properties. The results of studies of fatigue degradation caused by a constant direct/alternating electric field are often contradictory and ambiguous.[22–24] At the same time, it should be noted that the latter determines the reliability of the piezoelectric component used in various devices.

The mechanical properties of the indicated SS are also practically not studied. Considering their attractiveness for use in low-power linear and step motors, as well as medical diagnostic devices, it is relevant to dwell on this issue as well.

Taking into account the above, it is advisable to investigate the effect of electrical fatigue generated by an *ac* field on degradation properties, as well as to establish correlations between composition, structure, microstructure, mechanical strength of multicomponent ferroactive SS of the PZT–PZN–PMN system.[19]

§Corresponding author.

2. Materials and Methods

2.1. *Fabrication of samples*

The objects of study were SS of the PZT–PZN–PMN system modified by Ba and Sr, corresponding to the formula $(Pb_{1-\alpha_1-\alpha_2}Sr_{\alpha_1}Ba_{\alpha_1})$ $[Ti_xZr_y\{(Nb_{2/3}Zn_{1/3})$ $(Nb_{2/3}Mg_{1/3})\}_{1-x-y}]O_3$, with $\alpha_1 = 0.02 \div 0.12$; $\Delta\alpha_1 = 0.02$, $\alpha_2 = 0.0036 \div 0.073$; $x = 0.385 \div 0.430$, $y = 0.402 \div 0.447$. The most thoroughly studied SS with $\alpha_1 = 0.02$, $\alpha_1 = 0.10$, $\alpha_1 = 0.12$. The procedure for obtaining experimental samples is described in detail in Ref. 19.

2.2. *Methods of studying samples*

The study of the *P–E* dielectric hysteresis loops was carried out using the Sawyer–Tower circuit at $f = 50$ Hz, $T = 300$ K. The amplitude of the alternating voltage was set at the beginning of the study and then did not change during the entire experiment.

Compression strength tests were carried out on samples of various compositions in the form of disks. Sizes ranged from 10 to 12 mm. The loading of the thin disk occurred when it was fixed on an even base by a punch. The punch diameter was 5 mm. Loading took place on a special testing machine brand SHIMADZU. A special device provided coaxial axisymmetric application of forces along the axis of the cylinder. The loading speed of the sample was the same throughout the test time and was taken equal to 0.5 mm/min. The compressive stresses at the moment of fracture of the specimen, which are fixed by an abrupt increase in the strain of the specimen, in some cases, with the appearance of cracking (fragmentation), were taken as the strength value.

As a result of the tests, the characteristic forms of fracture of the samples were established: fragmentation into several fragments, spattering corresponding to samples with low strength, and separation of the sample by one crack passing through the center of fixation of the punch into two fragments. The latter type of failure corresponds to samples with high strength.

The ultimate stress during compression of thin samples was calculated by the formula $\sigma = (P \cdot k/S)$, where P is the force of punch loading, S is the area of the loading punch, k is the scale factor (by default, $k = 1$).

3. Experimental Results and Discussion

Figure 1, as an example, shows the *P–E* loops of SS with $\alpha_1 = 0.02$ and $x = 0.425$ at different numbers of repolarization cycles (n). It was found that all *P–E* loops have a form characteristic of classical ferroelectrics. An increase in n causes an expansion of the loops along the abscissa and a significant narrowing (almost twofold) along the ordinate.

Figure 2 shows the calculated parameters P_s, P_r, E_c from n. It was found that as n increases, the studied dependences have an almost linear form up to $n \sim 10^4$. A subsequent increase

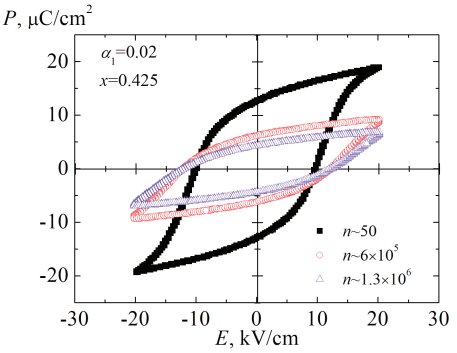

Fig. 1. *P–E* loops of SS with $\alpha_1 = 0.12$, $x = 0.390$ at $T = 300$ K.

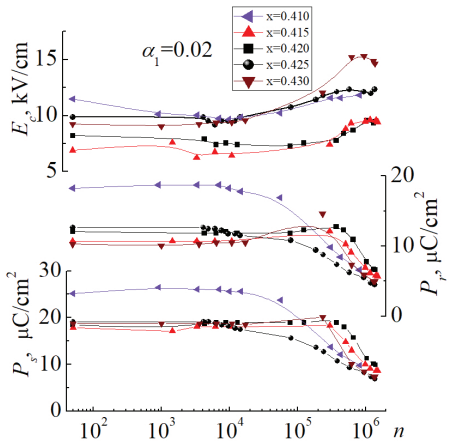

Fig. 2. Dependences of (P_s, P_r, E_c) on n of investigated SS with $\alpha_1 = 0.02$.

in n causes a slight increase in E_c and a decrease in P_s and P_r. For $n > 5 \times 10^5$, all x studied at $\alpha_1 = 0.02$ are characterized by a sharp increase in E_c and a decrease in P_s, P_r up to $n \sim 1.5 \times 10^6$.

Figure 3 shows the *P–E* loops of SS with $\alpha_1 = 0.10$ for different n. It is shown that the *P–E* loops have the form

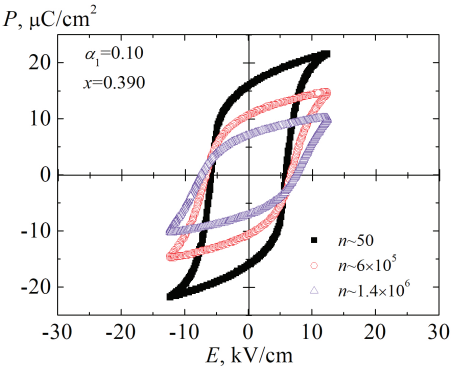

Fig. 3. *P–E* loops of SS with $\alpha_1 = 0.10$, $x = 0.390$ at $T = 300$ K.

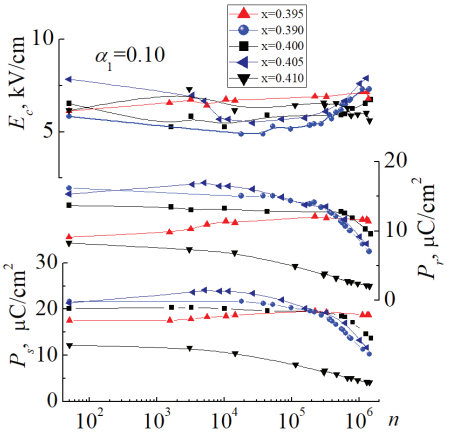

Fig. 4. Dependences of (P_s, P_r, E_c) on n of investigated SS with $\alpha_1 = 0.10$.

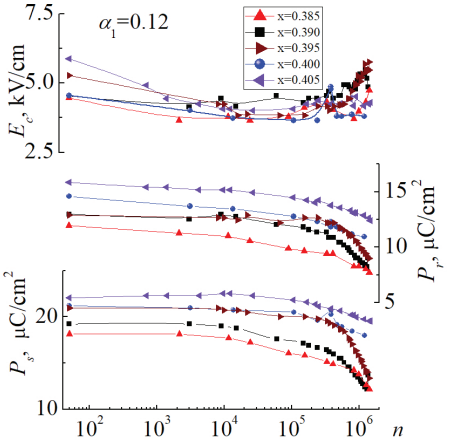

Fig. 6. Dependences of (P_s, P_r, E_c) on n of investigated SS with $\alpha_1 = 0.12$.

characteristic of classical ferroelectrics at small n. An increase in n led to a significant expansion of the loop along the abscissa axis and contraction along the ordinate axis for $n > 10^5$.

Figure 4 shows the dependences of the parameters P_s, P_r, E_c on n obtained in the SS with $\alpha_1 = 0.10$. It was revealed that, in the SS data, P_s, P_r practically do not change at $x < 0.410$ up to $n = 10^5$, deviating by several percent relative to the values obtained at $n < 10^2$. A decrease in the polarization parameters is observed at $n > 5 \times 10^5$.

At $x = 0.410$, these characteristics demonstrate stability at small numbers of repolarization cycles. A gradual increase in n leads to a decrease in P_s, P_r almost twofold, up to $n = 10^6$. For E_c in all investigated SS, at a given α_1, on the contrary, nonmonotonic behavior with the formation of extrema at $n < 5 \times 10^5$ is characteristic. Exceeding the specified n causes an increase in the specified characteristic.

Figure 5 shows the P–E loops of SS with $\alpha_1 = 0.12$ for different n. An increase in the Sr content in the investigated SS does not cause a qualitative change in the studied loops, the shape of which is also, as before, characteristic of classical ferroelectrics. It should be noted that at the indicated Sr content, P_s, P_r increase with Ti, in contrast to the investigated SS with $\alpha_1 < 0.12$.

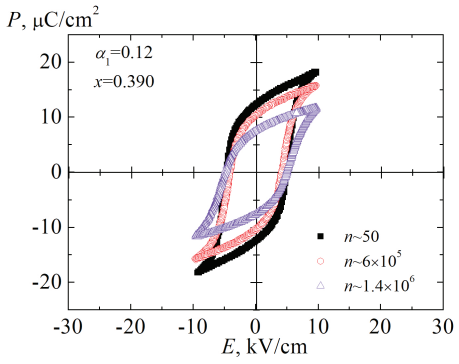

Fig. 5. P–E loops of SS with $\alpha_1 = 0.12$, $x = 0.390$ at $T = 300$ K.

Another distinctive feature is an increase in n as the Sr content increases, at which P_s decreases by about 50% and P_r by 25% (Fig. 6). The behavior of E_c is characterized by a decrease to ~3×10^4, after which a plateau-like section of the $E_c(n)$ dependence is formed to $n \sim 2 \times 10^5$. A further increase in n leads to a significant increase in the coercive fields with the formation of extrema at $n \sim 3 \times 10^5$.

The obtained dependences (P_s, P_r) (n) are in good agreement with the usually shown graph of the evolution of polarization versus the number of bipolar fatigue cycles in Fig. 7[25] and, probably, are caused either by the agglomeration of charges on internal barriers or domain walls, which causes an increase in the internal displacement field; or defective dipoles that reorient with respect to spontaneous polarization and, thereby, clamping the preferred orientation.

The analysis presented in Fig. 8 dependences of the mechanical strength, σ, and the average grain size, $\bar{D}$, SS of

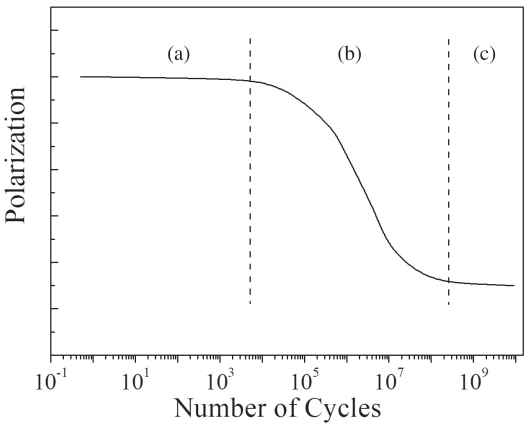

Fig. 7. Evolution of polarization with the number of bipolar fatigue cycles: (a) slow fatigue stage, (b) logarithmic stage, and (c) saturated stage.

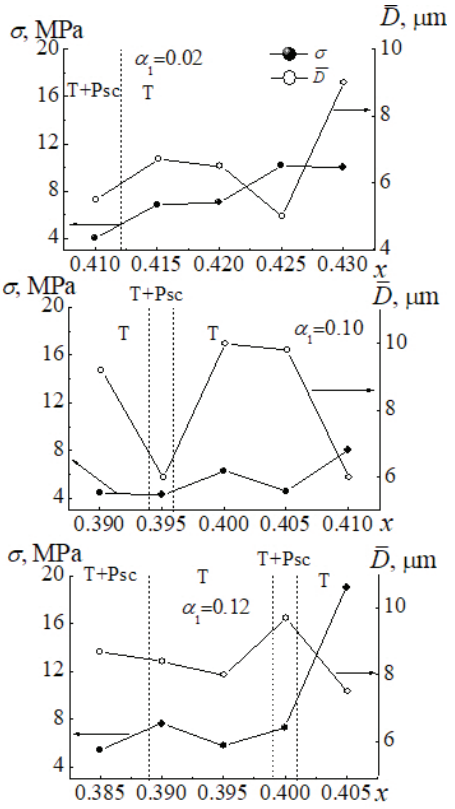

Fig. 8. Phase patterns and dependences of mechanical strength, σ average grain size, $\bar{D}^*$, SS of composition $(Pb_{1-\alpha_1-\alpha_2}Sr_{\alpha_1}Ba_{\alpha_1})[Ti_xZr_y\langle(Nb_{2/3}Zn_{1/3})(Nb_{2/3}Mg_{1/3})\rangle_{1-x-y}]O_3$, from the concentration of Ti (x) in the PZT–PZN–PMN system with different content of Sr (α_1) (*-by data[23]).

the composition on the concentration of Ti (x) in the PZT–PZN–PMN system showed a complete correlation of the "behavior" of σ with the change in $\bar{D}$:SS with a smaller size has a higher mechanical strength grains, characterized by a larger area of intergranular boundaries and, naturally, a larger area of grain contacts.

The latter is responsible for the greater hardening of fine-grained ceramics. We also note that, as in the case of the electrophysical characteristics,[19] the mechanical strength demonstrate some anomalies in the vicinity of structural instabilities accompanied by phase transitions.

4. Conclusion

The electrical fatigue and mechanical strength of SS of the PZT–PZN–PMN system, modified with Ba and Sr, corresponding to the formula $(Pb_{1-\alpha_1-\alpha_2}Sr_{\alpha_1}Ba_{\alpha_1})[Ti_xZr_y\langle(Nb_{2/3}Zn_{1/3})(Nb_{2/3}Mg_{1/3})\rangle_{1-x-y}]O_3$. It is shown that the evolution of polarization characteristics with an increase in the number of cycles is consistent with the data presented in the literature and is characterized by two sections: the stage of slow fatigue and the logarithmic stage. An increase in the strontium content shifts the beginning of the logarithmic stage towards large n. The study of mechanical strength showed a decrease in σ with an increase in the average grain size. It is advisable to use the obtained data in the development of devices operating in power modes.

Acknowledgments

The study was carried out with the financial support of the Ministry of Science and Higher Education of the Russian Federation (State task in the field of scientific activity, scientific project No. (0852-2020-0032)/(BAZ0110/20-3-07IF). The equipment of the Center of Research Institute of Physics SFedU was used.

References

[1]H. Yagubizade, M. Darvishi, M. C. Elwenspoek and N. R. Tas, A UHF 4th-order band-pass filter based on contour-mode PZT-on-Silicon resonators, *2014 IEEE 27th Int. Conf. Micro Electro Mechanical Systems (MEMS)* (2014), pp. 1237–1240, doi:10.1109/MEMSYS.2014.6765872.

[2]H. Chandrahalim, S. A. Bhave, R. G. Polcawich, J. S. Pulskamp and R. Kaul, PZT transduction of high-overtone contour- mode resonators, *IEEE Trans. Ultrason., Ferroelectr. Freq. Control* **57**(9), 2035 (2010), doi:10.1109/TUFFC.2010.1651.

[3]S. Hayashi and Y. Sasaki, Rapid tracking of resonance and antiresonance of a piezoelectric reasonator: A phase-locked loop for capacitive loads, *Jpn. J. Appl. Phys.* **30**, 132 (1991), doi:10.7567/JJAPS.30S1.132.

[4]M. A. Popov, I. V. Zavislyak, P. Zhou, T. Li, P. J. Shah, B. M. Howe, M. E. McConney, G. Srinivasan and M. R. Page, An electric field controlled dual resonator magneto-electric band-stop filter, *Microw. Opt. Technol. Lett.* **61**, 873 (2019), doi:10.1002/mop.31679.

[5]M. Zheng, S. Zhou and M. Tomizuka, Identification of resonance frequencies in dual-stage hard disk drives: A practical strategy, *Proc. ASME 2017 Dynamic Systems and Control Conf.* (2017) V002T23A001, doi:10.1115/DSCC2017-5096.

[6]M. Haq, Application of piezo transducers in biomedical science for health monitoring and energy harvesting problems, *Mater. Res. Express* **6**, 022002 (2019), doi:10.1088/2053-1591/aaeffb8.

[7]G. Frit, C. Wang, P. Kumar, S. Singh, J. Ryu and S. Priya, Effect of sintering temperature and packing powder on the properties of Pb (Zr, Ti, Mg, Zn, Nb)O_3 ceramic, *Jpn. J. Appl. Phys.* **42**, L595 (2003), doi:10.1143/JJAP.42.L595.

[8]M. Kobune, Y. Tomoyoshi, A. Mineshige and S. Fujii, Effects of MnO_2 addition on piezoelectric and ferroelectric properties of $PbNi_{1/3}Nb_{2/3}O_3$–$PbTiO_3$–$PbZrO_3$ ceramics, *J. Ceram. Soc. Jpn.* **108**, 633 (2000).

[9]Q. Sun and T. Liu, Effects of dopants on properties of PZN-PSN-PMN-PZT ceramics, *J. Wuhan Univ. Technol., Mater. Sci. Ed.* **20**, 20 (2005), doi:10.1007/BF02841267.

[10]Y. Gao, Y.-H. Chen, J. Ryu, K. Uchino and D. Viehland, Eu and Yb substituent effects on the properties of $Pb(Zr_{0.52}Ti_{0.48})O_3$–$Pb(Mn_{1/3}Sb_{2/3})O_3$ ceramics: Development of a new high-power piezoelectric with enhanced vibrational velocity, *Jpn. J. Appl. Phys.* **40**, 687 (2001), doi:10.1143/jjap.40.687.

[11]C. H. Wang, S. J. Chang and P. C. Chang, Effect of sintering conditions on characteristics of $PbTiO_3$–$PbZrO_3$–$Pb(Mg_{1/3}Nb_{2/3})O_3$–$Pb(Zn_{1/3}Nb_{2/3})O_3$, *Mater. Sci. Eng.: B* **111**, 124 (2004), doi:10.1016/j.mseb.2004.03.028.

[12]G. H. Haertling, Ferroelectric ceramics: History and technology, *J. Am. Ceram. Soc.* **82**, 797 (1999), doi:10.1111/j.1151-2916.1999.tb01840.x.

[13]M. V. Talanov, A. A. Pavelko, L. A. Reznichenko, Y. N. Zakharov, A. G. Lutokhin and A. V. Turik, E-T phase diagrams of a solid solution of the multicomponent $PbZn_{1/3}Nb_{2/3}O_3$–$PbMg_{1/3}Nb_{2/3}O_3$–$PbNi_{1/3}Nb_{2/3}O_3$–$PbTiO_3$ system near the morphotropic phase boundary, *Phys. Solid State* **56**, 612 (2014), doi:10.1134/S1063783414030330.

[14]A. A. Pavelko and L. A. Reznichenko, Piezodielectric properties of PMN–PZT–PT solid solutions under the action of high temperatures, *Bull. Russ. Acad. Sci.: Phys.* **78**, 802 (2014), doi:10.3103/S1062873814080280.

[15]J. Gao, W. Ma, Y. Yang, J. Guo, H. Zhao and M. Ma, The free-standing multilayer thick films of $0.7Pb(Zr_{0.46}Ti_{0.54})O_3$–$0.1Pb(Zn_{1/3}Nb_{2/3})O_3$–$0.2Pb(Ni_{1/3}Nb_{2/3})O_3$ with low co-fired temperature, *J Mater Sci: Mater Electron.* **29**, 11664 (2018), https://doi.org/10.1007/s10854-018-9263-1.

[16]K. P. Andryushin, I. N. Andryushina, L. A. Shilkina, A. V. Nagaenko, S. I. Dudkina, A. A. Pavelko, I. A. Verbenko and L. A. Reznichenko, Features of the structure and macro responses in hard ferro piezoceramics based on the PZT system, *Ceram. Int.* **44**, 18303 (2018), doi:10.1016/j.ceramint.2018.07.042.

[17]L. A. Reznichenko, I. A. Verbenko, L. A. Shilkina, A. V. Pavlenko, S. I. Dudkina *et al.*, Binary, ternary and four-component systems based on sodium niobate: Phase diagrams of states, the role of the number of components and defectiveness in the formation of the properties, *Int. Conf. Physics, Mechanics of New Materials and Their Applications, PHENMA 2017* (2018), pp. 3–23, doi:10.1007/978-3-319-78919-4_1.

[18]R. Muanghlua, S. Niemchareon, W. C. Vittayakorn and N. Vittayakorn, Effects of Zr/Ti ratio on the structure and ferroelectric properties in PZT-PZN-PMN ceramics near the morphotropic phase boundary, *Adv. Mater. Res.* **55–57**, 125 (2008), doi:10.4028/www.scientific.net/AMR.55-57.125.

[19]K. P. Andryushin, L. A. Shilkina, I. N. Andryushina, A. V. Pavlenko, A. V. Nagaenko, I. A. Verbenko and L. A. Reznichenko, Multi component ferroactive materials for low-frequency applications: Features of the crystal and grain structure, macro-responses, *Ceram. Int.* **45**, 16855 (2019), doi:10.1016/j.ceramint.2019.05.228.

[20]J. S. Han, C. W. Gal, J. M. Park and S. J. Park, Powder injection molding of PNN-PMN-PZN doped low temperature sintering PZT ceramics, *J. Manuf. Process.* **28**, 235 (2017), doi:10.1016/j.jmapro.2017.06.008.

[21]L. D. Vuong, P. D. Gio, N. D. V. Quang, T. D. Hieu and T. P. Nam, Development of $0.8Pb(Zr_{0.48}Ti_{0.52})O_3$–$0.2Pb[(Zn_{1/3}Nb_{2/3})_{0.625}(Mn_{1/3}Nb_{2/3})_{0.375}]O_3$ ceramics for high-intensity ultrasound applications, *J. Electron. Mater.* **47**, 5944 (2018), doi:10.1007/s11664-018-6454-8.

[22]X. J. Lou, Polarization fatigue in ferroelectric thin films and related materials, *J. Appl. Phys.* **105**, 024101 (2009), https://doi.org/10.1063/1.3056603.

[23]Q. Y. Jiang, E. C. Subbarao and L. E. Cross, Effect of composition and temperature on electric fatigue of La-doped lead zirconate titanate ceramics, *J. Appl. Phys.* **75**, 7433 (1994), https://doi.org/10.1063/1.356637.

[24]C. Wang, C. He, Z. Wang, X. Li, X. Yang, Y. Liu and X. Long, Fatigue endurance enhancement of Sn-doped $Pb(Lu_{1/2}Nb_{1/2})O_3$–$PbTiO_3$ ceramics, *RSC Adv.* **8**, 11633 (2018), doi:10.1039/c8ra00732b.

[25]T. Mihara and H. W. Paz de Araujo, Polarization fatigue characteristics of sol-gel ferroelectric $Pb(Zr_{0.4}Ti_{0.6})O_3$ thin-film capacitors, *Jpn. J. Appl. Phys.* **33**, 3996 (1994), https://doi.org/10.1143/JJAP.33.3996.